



Alternative Functional *rad21* Paralogs in *Fusarium oxysporum*

Manish Pareek¹, Yael Almog¹, Vinay Kumar Bari¹, Einat Hazkani-Covo², Itay Onn³ and Shay Covo^{1*}

¹ Department of Plant Pathology and Microbiology, The Robert H. Smith Faculty of Agriculture, Food and Environment, The Hebrew University of Jerusalem, Rehovot, Israel, ² Department of Natural Sciences, Open University of Israel, Ra'anana, Israel, ³ The Azrieli Faculty of Medicine, Bar Ilan University, Safed, Israel

OPEN ACCESS

Edited by:

Weiguo Fang,
Zhejiang University, China

Reviewed by:

Kaustuv Sanyal,
Jawaharlal Nehru Centre
for Advanced Scientific Research,
India
Irene Castano,
Instituto Potosino de Investigación
Científica y Tecnológica (IPICYT),
Mexico

*Correspondence:

Shay Covo
shay.covo@mail.huji.ac.il

Specialty section:

This article was submitted to
Fungi and Their Interactions,
a section of the journal
Frontiers in Microbiology

Received: 24 October 2018

Accepted: 31 May 2019

Published: 18 June 2019

Citation:

Pareek M, Almog Y, Bari VK,
Hazkani-Covo E, Onn I and Covo S
(2019) Alternative Functional *rad21*
Paralogs in *Fusarium oxysporum*.
Front. Microbiol. 10:1370.
doi: 10.3389/fmicb.2019.01370

Cohesin, the sister chromatid cohesion complex, is an essential complex that ensures faithful sister chromatid segregation in eukaryotes. It also participates in DNA repair, transcription and maintenance of chromosome structure. Mitotic cohesin is composed of Smc1, Smc3, Scc3, and Rad21/Mcd1. The meiotic cohesin complex contains Rec8, a Rad21 paralog and not Rad21 itself. Very little is known about sister chromatid cohesion in fungal plant pathogens. *Fusarium oxysporum* is an important fungal plant pathogen without known sexual life cycle. Here, we describe that *F. oxysporum* encodes for three Rad21 paralogs; Rad21, Rec8, and the first alternative Rad21 paralog in the phylum of ascomycete. This last paralog is found only in several fungal plant pathogens from the Fusarium family and thus termed *rad21nc* (non-conserved). Conserved *rad21* (*rad21c*), *rad21nc*, and *rec8* genes are expressed in *F. oxysporum* although the expression of *rad21c* is much higher than the other paralogs. *F. oxysporum* strains deleted for the *rad21nc* or *rec8* genes were analyzed for their role in fungal life cycle. $\Delta rad21nc$ and $\Delta rec8$ single mutants were proficient in sporulation, conidia germination, hyphal growth and pathogenicity under optimal growth conditions. Interestingly, $\Delta rad21nc$ and $\Delta rec8$ single mutants germinate less effectively than wild type (WT) strains under DNA replication and mitosis stresses. We provide here the first genetic analysis of alternative *rad21nc* and *rec8* paralogs in filamentous fungi. Our results suggest that *rad21nc* and *rec8* may have a unique role in cell cycle related functions of *F. oxysporum*.

Keywords: cohesin, Mcd1, Rad21, Rec8, *Fusarium oxysporum*, cell cycle

INTRODUCTION

Fusarium oxysporum is a soil-borne plant pathogen that infects more than hundred plant species and causes severe yield losses (Dean et al., 2012). *F. oxysporum* has polyphyletic origin with lineage-specific chromosomes that encode for pathogenicity genes (Ma et al., 2010, 2013). These lineage specific chromosomes are mobile; they can be transferred between isolates passaging pathogenic traits (Ma et al., 2010). In addition, *F. oxysporum* is capable of exchanging segments of chromosomes between isolates although a sexual life cycle was never identified. This suggests that parasexual recombination does occur in this fungus (Vlaardingerbroek et al., 2016). Very little is known about chromosome transmission and parasexual recombination at the mechanistic level in *F. oxysporum*. The motivation of this study is to identify *F. oxysporum*-specific chromosomal

proteins. The long term goal is to assess the role of these proteins in chromosome transactions that may specifically occur in *F. oxysporum*. A small scale comparative genomic study led us to focus on the cohesin complex.

The cohesin complex consists of Smc1, Smc3, Rad21 (also known as Mcd1 or Scc1), and Scc3 (Onn et al., 2008; Nasmyth and Haering, 2009). In the meiotic cohesin complex, the Rad21 subunit is replaced by its meiosis specific paralog Rec8 (Bhatt et al., 1999; Watanabe and Nurse, 1999). From an evolutionary standpoint the cohesin complex is part of a broad family of proteins found in prokaryotes and eukaryotes containing the SMC motives. In the cohesin family of proteins; the kleisin subunit bridges between the two SMC subunits (Nasmyth and Haering, 2005; Gligoris et al., 2014; Palecek and Gruber, 2015). There are several kleisin families; here we focus on α -kleisins that are part of the cohesin complex (Nasmyth and Haering, 2005). The α -kleisins subunits connect Smc1 and Smc3 by binding their globular heads. In yeast, the Mcd1 (Rad21) N-terminal is bound to Smc3 and the C-terminal to Smc1 (Haering et al., 2002). Besides binding Smc1 and Smc3 in eukaryotes α -kleisins contain separase cleavage sites that allow destruction of the cohesin complex in anaphase (Uhlmann et al., 1999). The cohesin complex holds the newly replicated sister chromatids till anaphase thus it ensures the proper segregation of chromatids (Spencer et al., 1990; Guacci et al., 1997; Onn et al., 2008; Covo et al., 2012, 2014). Cohesin also has an important role in determining the efficiency and fidelity of homologous recombination by facilitating recombination between sister chromatids and excluding recombination between homologous chromosomes (Sjögren and Nasmyth, 2001; Ünal et al., 2004; Covo et al., 2010). During meiosis, an alternative form of cohesin is formed that functions in a different way; meiotic cohesins suppress recombination between sister chromatids and facilitate recombination between homologous chromosomes (Zickler and Kleckner, 1999; Kim et al., 2010).

Cohesin also functions in transcription regulation of mRNA and rRNA (Lengronne et al., 2004; Bose and Gerton, 2010). It has a major role in maintaining 3D chromatin structure by supporting chromatin loops formations that bring distal genome parts together (Kagey et al., 2010; Li et al., 2013; Kakui and Uhlmann, 2018; van Ruiten and Rowland, 2018 and the references therein).

All the subunits of cohesin are well conserved across eukaryotes, however, there are several examples of lineage-specific gene duplication of some subunits. In *Arabidopsis thaliana* two *RAD21* paralogs (*AtRAD21.2/SYN3* and *AtRAD21.3/SYN4*) have a role in somatic DNA double strand break repair (Dong et al., 2001; da Costa-Nunes et al., 2006, 2014; Bolaños-Villegas et al., 2017). In addition, *SYN1* encodes for a Rad21/Rec8 like protein that functions in meiosis. *Arabidopsis SYN1* gene mutants are male and female sterile, defective in chromosome condensation and pairing start at leptotene stage of meiosis I. *SYN1* is dispensable for somatic and vegetative growth though (Bai et al., 1999; da Costa-Nunes et al., 2014). *DIF1* is another *Arabidopsis* homolog of Rec8/Rad21, mutants are completely male and female sterile and showed multiple meiotic defects in *Arabidopsis* (Bhatt et al., 1999).

In *Caenorhabditis elegans* and mammals, it was shown that at least two *RAD21/REC8* paralogs function in a non-redundant manner in meiosis (Severson et al., 2009; Ishiguro et al., 2011; Severson and Meyer, 2014). In conclusion, all reported Rad21 paralogs were shown to be functional. To the best of our knowledge, only two Rad21 paralogs were reported in fungi, the mitotic Rad21 and the meiotic Rec8. Interestingly, even fungi without known sexual life cycle like *F. oxysporum* encode for *rec8*. Here, we report that three paralogs of *rad21* are encoded in the genome of *F. oxysporum*. One is the conserved, canonical *rad21* (*rad21c*), another is a non-conserved *rad21* (*rad21nc*) and a meiotic specific, i.e., *rec8*. Based on genetic analysis of *rad21nc* and *rec8* paralogs in *F. oxysporum* we suggest that the alternative paralogs are also functional and they may have a Fusarium-specific function in cell cycle regulation.

MATERIALS AND METHODS

Phylogenetic Analysis of the *rad21* Paralogs

Protein sequences were collected from 12 fungal species for *rad21* paralogs and analyzed; the orthologous were aligned using MAFFT v7.221 (Katoh et al., 2009) with default parameters for protein alignment. Guidance2 was used to remove untrustable positions from the alignment with a Guidance score below 0.93 (Sela et al., 2015). A phylogenetic tree with 100 bootstrap replicates was then reconstructed using RAxML v8.2.11 (Stamatakis, 2014) with GAMMA model of rate heterogeneity (Yang, 1994) and the GTR substitution model. Species tree was reconstructed by 90 DNA Repair proteins listed in **Supplementary Table S1**.

Analysis of Rad21nc Sequence and Predicted Structures

Sequence alignments were done with ClustalX2 (Larkin et al., 2007). Structural prediction was done by using I-TASSER (Zhang, 2008; Roy et al., 2010; Yang et al., 2015) PDB 1W1W and 4UX3 were assigned as modeling templates for *F. oxysporum* Rad21nc sequence (Haering et al., 2004; Gligoris et al., 2014).

Fungal Strain and Culture Conditions

All experiments described here used *F. oxysporum* f. sp. *lycopersici* strain 4287 (Fungal Genetics Stock Center #9935). Glycerol stock of original fungal strain is maintained at -80°C . For spore isolation, spores were inoculated in 50 ml in KNO_3 (1.36 gm yeast nitrogen base, 24 gm sucrose, 100 mM KNO_3 in 800 mL distilled water) medium in Erlenmeyer flask and incubated in 28°C at 250 rpm for 4–6 days. The mycelia/spore suspension was then filtered using a cell strainer (40 μm , SPL Life Sciences, South Korea), the filtrates were centrifuged and washed twice with distilled water. Spores were diluted and counted using a Neubauer counting chamber. Spores and mycelia were also grown on potato dextrose agar (PDA) plates and incubated at 28°C for 5–7 days for various experiments.

RT-PCR and qPCR Expression Analysis for *rad21* Paralogs

RT-PCR was performed to quantify the expression of the different *rad21* paralogs in WT and mutant strains. RNA was isolated from spores 8 h post inoculation using Plant RNAeasy kit (Qiagen, United States). Then, cDNA was made by FastQuant RT Kit (Tiangen Biotech, China). Further, *rad21* paralogs and *act1* (*actin*) genes were amplified using specific primers (P16 to P23) described in **Supplementary Table S2**. SYBR green (Thermo Fisher Scientific, United States) was used for qPCR analysis using StepOnePlus™ Real-time PCR system (Applied Biosystems, United States).

To analyze the effect of cell cycle arrest on the expression of *rad21* paralogs fungal spores (0.2 billion) germinated in 10 mL of potato dextrose broth (PDB) with or without 100 mM hydroxyurea (HU) or 50 µg/mL benomyl for 14 h at 28°C, 250 rpm. RNA isolation and cDNA preparation was done as described above. *act1* gene served as an internal control. Fold change were calculated relative to PDB germinated spores using the $\Delta\Delta C_T$ method (Livak and Schmittgen, 2001).

Generation of $\Delta rad21nc$ or $\Delta rec8$ Strains

The deletion constructs for *F. oxysporum rad21nc* or *rec8* genes were prepared using the split marker approach as previously described, with few modifications (Catlett et al., 2003; Yu et al., 2004). The strategy for preparation of the split cassette is described in **Supplementary Figure S1**. Briefly, 620 bp upstream flanking region and 672 bp long downstream region of *rad21nc* coding region (FOXG_15850) were amplified from *F. oxysporum* genomic DNA using primers P1/P2 and P3/P4, respectively (**Supplementary Table S2**). Hygromycin cassette (HYG) was amplified using primers P5/P6 from pSilent-1 vector (Fungal Genetics Stock Center, Manhattan, KS, United States) (Nakayashiki et al., 2005). Further combined region with upstream *rad21nc* and a half portion of HYG cassette (Split 1) was amplified using nested primer P7/P8. Similarly, fragment combining downstream *rad21nc* and the other half of the HYG cassette (Split 2) were prepared using primers P9/P10. For, *rec8* (FOXG_03390) same strategy was used for preparation in split 1 and split 2 cassettes. The primers used were enlisted in the **Supplementary Table S2**. For, random HYG (hygromycin B phosphotransferase) transformants full length HYG gene along with *trpC* promoter and terminator was amplified from pSilent1 using primers (P14 and P15).

Fusarium oxysporum protoplast preparation and PEG mediated transformation were done as described before (Di Pietro et al., 1998; Bae and Knudsen, 2000; Moradi et al., 2013; Ramamoorthy et al., 2015). Around 0.2–0.8 million protoplasts were mixed with ~10 µg DNA of each cassette (split 1 and split 2). For fungal transformants selection top water agar layer was used with Hygromycin-B at final concentration 100 µg/mL. Transformation plates were kept for 4–5 days for transformants to appear. Each putative transformant was grown on PDB and conidia were spread again on selection plate to obtain monoconidial culture. Selected fungal transformants were screened using primers that amplify the full length of the target gene (primers P11/P12). Amplification of the *rad21nc/rec8*

ORF fragment using P1/P11 and P13 primers was also done for further confirmation. In this case, true mutants do not show amplification of PCR product (**Supplementary Figures S3, S4**). Confirmed transformants were stored at –80°C and used for further experiments.

Phenotypic Analysis for the *rad21nc* and *rec8* Mutants

To analyze the effect of different stress conditions on radial growth, equal size of mycelial agar plugs from each mutant culture were inoculated on PDA plates. The plates were incubated at 28°C for 3 days and then the diameter was measured. For sporulation analysis, mycelial agar plugs from WT and mutant cultures were inoculated in 5 mL PDB and incubated for 6 days at 28°C with shaking at 250 rpm. Spores were filtered and counted using a Neubauer counting chamber.

Measurement of the Effect of Chromosome Stressors on Fungal Cultures

To measure the effect of hydroxyurea (HU) or benomyl on germination of WT and mutant strains, spores were isolated from the cultures grown on PDA plates at 28°C for 5–7 days by mere scrubbing of mycelia in 5 ml of water. Crude spore suspension was filtered, washed and dissolved in 1 ml of water. Spores were then inoculated for 14 h in PDB with or without treatment at 28°C, 250 rpm. The germinated spores were microscopically analyzed, using the five locations on a single side. Germinated and ungerminated spores were counted with the help of ImageJ software (Schneider et al., 2012). Experiments were repeated three times.

To measure the effect of DNA damage on colony formation of the different strains, conidia were pronged with serial dilutions onto PDA plates containing 0.01% of methyl methanesulfonate (MMS).

Tomato Plant Infection Assays

Tomato seedling infection assays were conducted as described (Di Pietro et al., 1998, 2001) with some modifications. 15 days old tomato seedlings [Rehovot-13; (Katan and Ausher, 1974)] were dipped in 5×10^6 spore per mL solution or in sterile water (mock) for 20 min. Then, plants were replanted in sterile soil-vermiculite mixture (60:40) and grown in a plant growth chamber at controlled growth conditions (25°C; ~80% humidity; 14/10 h. light/dark cycle). Plants were monitored on a daily basis; survivors and dead plants were counted after 21 days post inoculation (dpi). Fisher's exact test (two tailed) was used to assess the significance between the populations.

RESULTS

Identifying Three *rad21* Paralog in *Fusarium* Species

Initially, comparative genomics was used to identify *F. oxysporum* orthologs of proteins involved in DNA repair, recombination

and chromosome transmission. *Saccharomyces cerevisiae* and *Aspergillus nidulans* proteins were collected from previously published sources (Goldman and Kafer, 2004; Stirling et al., 2011). We first identified orthologs of these genes in *Neurospora crassa* due to the quality of annotation and its short phylogenetic divergence time from the *Fusarium* genus. Then, we used the *N. crassa* genes as seeds for BLASTP search in *F. oxysporum*. The BLASTP analysis of the *N. crassa* Rad21 protein against the proteome of *F. oxysporum* resulted in two paralogs with very high homology (E -value $< 10^{-153}$) and another one that showed lower homology (E -value $< 10^{-10}$). The two hits with the highest homology were the evolutionary conserved Rad21 and a never described before Rad21 paralog (FOXG_15850). The third paralog was Rec8. Rad21nc is not found in the closely related species to *F. oxysporum* and in other hypocreales but is found in *Fusarium solani* (XP_003044011), *Stachybotrys chartarum* (S7711_01263), *Stachybotrys chloronata*, and *Fusarium nygamai* (FNYG_15271) for this reason it was termed *rad21* non-conserved (*rad21nc*) (Figure 1A). To reveal the origin of Rad21nc we built a phylogenetic tree of Rad21 paralogs from several species in sordariomycetes. The Rad21 phylogenetic tree suggests that *rad21* gene duplication occurred after the divergence of *Trichoderma reesei* from the common ancestor of *Fusarium*, *Stachybotrys*, and *F. solani*. The duplication was followed by deletions of the gene that can not be found in *F. proliferatum*, *F. verticillioides*, and *F. graminearum*. An alternative, more complex, scenario is that the *rad21nc* gene was horizontally transferred from the branch of *Stachybotrys* to the branch of *Fusarium* species and then was lost from some of the *Fusarium* species. This scenario is supported by the fact that the *rad21nc* orthologs of *Stachybotrys* species are placed internally and not externally to branch of the *Fusarium* species (Figure 1A). Due to the low bootstrap values it is unclear if this is indeed the scenario (Figure 1A). In addition, the species tree that we built based on 90 genes (Supplementary Table S1) shows a slightly different phylogeny, especially with the placement of *T. reesei* and that of the *Stachybotrys* species. Therefore, it is hard to determine if indeed the gene duplication occurred after the divergence of *T. reesei*. This ambiguity is reflected in the low bootstrap values of the hypocreales tree as determined by other methods (Hongsanan et al., 2017). In any event, it is expected that *rad21nc* was found at the common ancestor of the *Fusarium* species. The most parsimonious evolutionary trajectory is that the *rad21nc* paralog was lost from most of the *Fusarium* species based on the fact that the Rad21nc sub-tree reflects the phylogenetic order of the species that contain the paralog (Figures 1A,B).

Comparison of Rad21c and Rad21nc Protein Sequence With Yeast ScMcd1 (ScRad21)

rad21nc is located on chromosome 8 of *F. oxysporum* f. sp. *lycopersici*; it is not part of the lineage specific loci of *F. oxysporum* f. sp. *lycopersici* and indeed the gene is encoded in all tested *F. oxysporum* spp. The gene, including UTR, is 2116 bp. The coding sequence is 1627 long bp and includes one 66 bp long intron. After examining all possible reading frames, we could

not find out any known domain encoded within the intron. The sequences of Rad21 and Rad21nc were compared. Rad21nc is 97 amino acids shorter than the canonical Rad21 (Figure 2A and Supplementary Figure S2). The size difference between Rad21 and Rad21nc is due to several short internal gaps and a ~30 amino acids C-terminal truncation. InterPro motif search revealed the characteristic Rad21/Rec8-like protein, N-terminal domain (IPR006910, a.a 1-82) and a winged helix DNA-binding domain (IPR036390, a.a 485-519) that mediate the interaction with Smc1 and Smc3, respectively, are marked by black line (Figure 2A). The interaction regions with Pds5 and Scc3 are also conserved while the sequence similarity outside these regions is lower (Figure 2B). Interestingly, scanning of Rad21nc against Eukaryotic Linear Motif resource (ELM) failed to identify the consensus separase cleavage motif. However, there are several partial motifs which may be recognized by the *F. oxysporum* separase protein. Based on the protein sequence, the structure of the N' and C' terminal domains of the Rad21nc protein were predicted by using the I-TASSER server. The predicted structure was aligned to the solved structures of *S. cerevisiae* Smc1 and Smc3 head domains that contain a N-terminal fragment of *S. cerevisiae* Mcd1 (Rad21). The structure of the N-terminal of Rad21nc is very similar to the ScMcd1 and completely overlaps with the ScMcd1 (Figure 2C). The Rad21nc C-terminal domain contains regions with uncertain folding. However, the helix that docks Rad21nc into Smc3 is well defined and properly localized into the coiled coil domain, when aligned to the solved structure of *S. cerevisiae* Smc3 with a C-terminal fragment of ScMcd1 (Figure 2D). This sequence and structural analysis suggest that the fold of Rad21nc N' and C' terminal domain is similar to other kleisins and that the Rad21nc can most likely form a complex with Smc1 and Smc3 cohesin subunits.

The RNA Expression of *rad21c* Gene Is Much Higher Than Both *rad21nc* and *rec8* Under All Tested Conditions

Next, we examined if the different *rad21* paralogs were expressed. RNA was purified from germinated spores of *F. oxysporum* f. sp. *lycopersici* and cDNA was prepared as described in the Section "Materials and Methods." The cDNA was then amplified with paralog-specific primers. Figure 3A shows amplification of all three paralogs. Yet, quantitative assessment using qPCR of the different transcripts revealed that the expression of the *rec8* and *rad21nc* genes was 3% and even lower in comparison with *rad21c* (Figure 3B).

We have also analyzed the RNA expression of *rad21* paralogs under HU or benomyl stress relative to PDB grown spores. qPCR analysis showed that *rad21c*, *rad21nc*, and *rec8* expression was slightly induced following benomyl stress (Figure 4). The expression of *rad21c* was still much higher under treated condition relative to *rad21nc* or *rec8*.

Hyphal Growth and Sporulation in the $\Delta rad21nc$ or $\Delta rec8$ Mutant Strains

Split marker approach was used to construct deletion cassettes for *rad21nc* or *rec8* genes as described in the Section "Materials

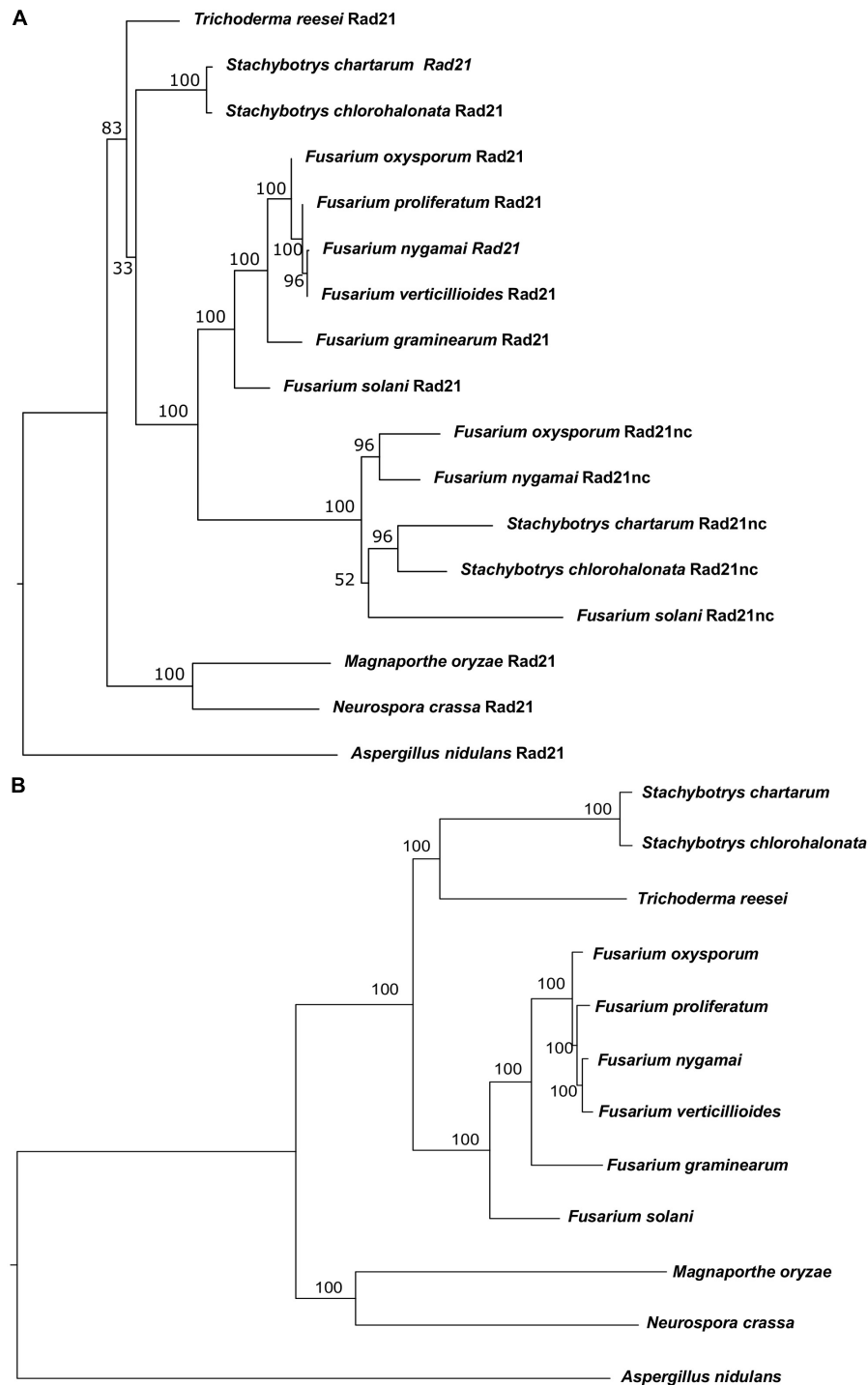
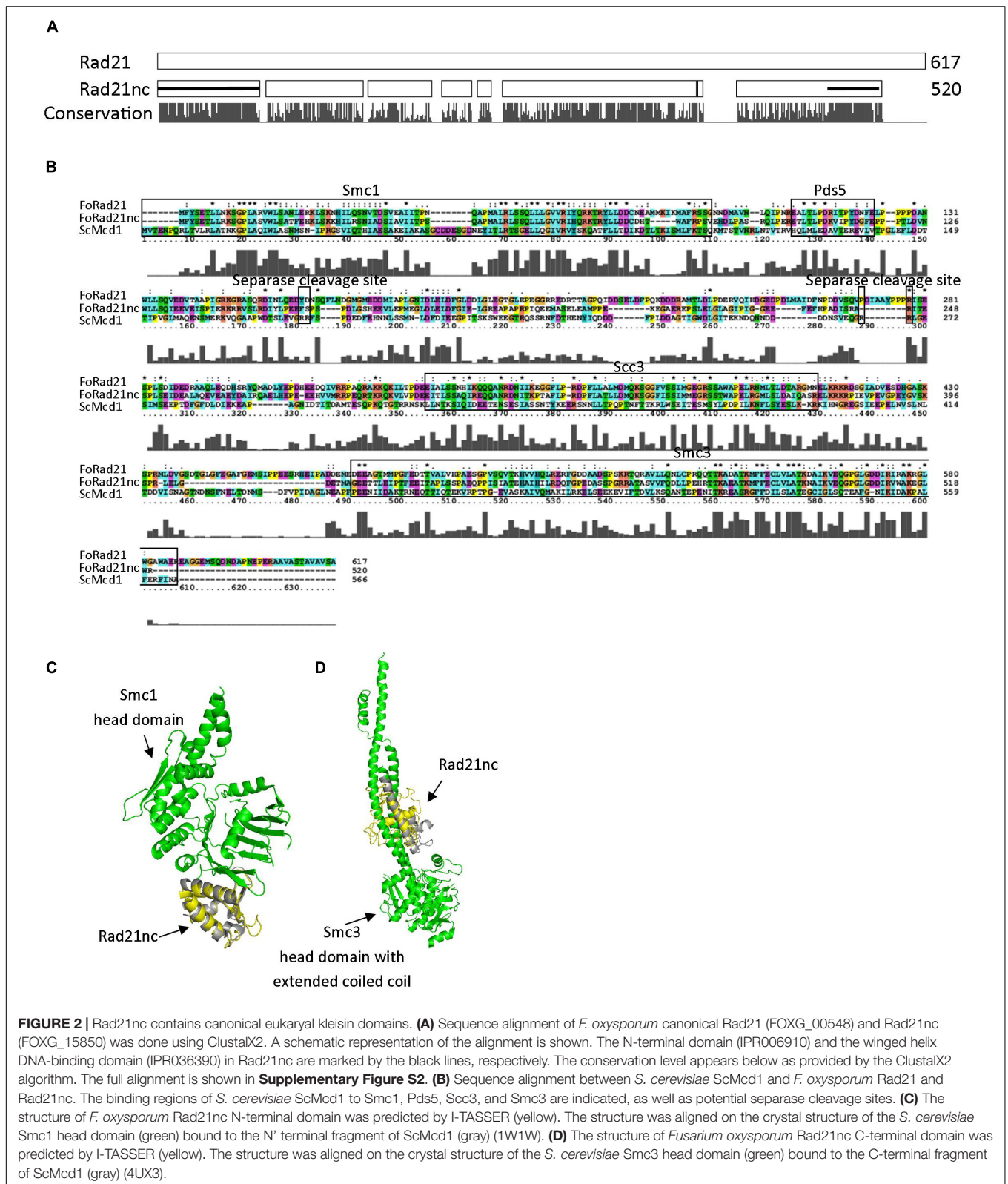


FIGURE 1 | Phylogenetic analysis of Rad21 paralogs in Sordariomycetes. **(A)** Phylogenetic analysis of the protein sequences of *rad21* orthologs and paralogs from selected sordariomycetes fungi with *Aspergillus nidulans* serves as an outgroup of sordariomycetes. *N. crassa* and *Magnaporthe oryzae* serve as outgroup species for hypocreales. The tree was constructed as described under the Section “Materials and Methods.” **(B)** The phylogenetic tree of the species that were used to reconstruct the Rad21 tree was built using the genes described in **Supplementary Table S1** as described in the Section “Materials and Methods.”

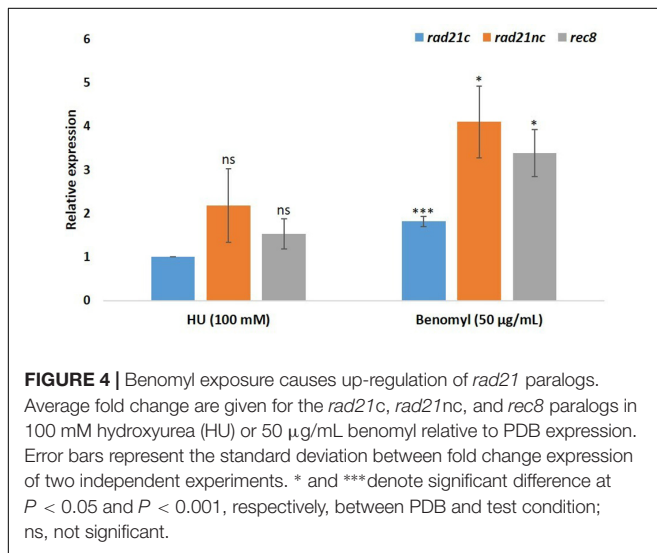
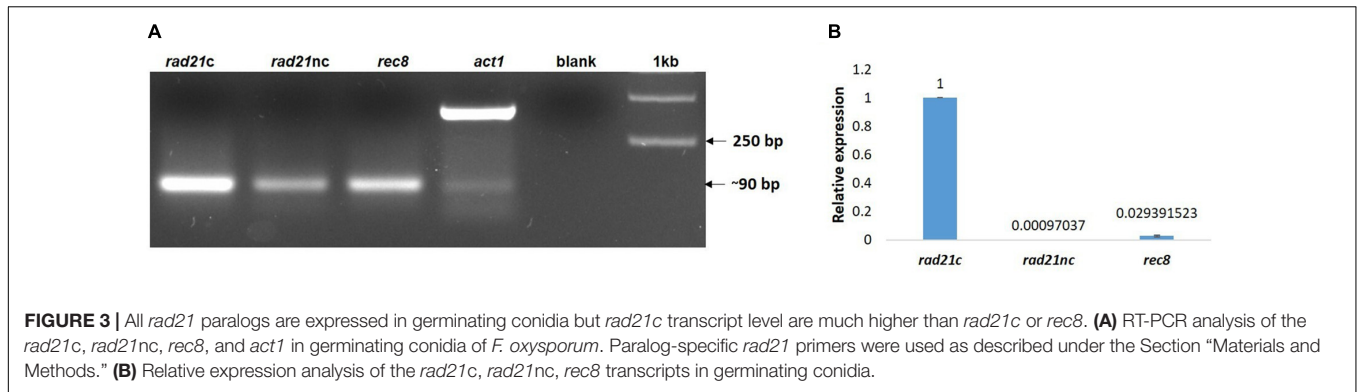
and Methods.” Transformants were selected on hygromycin containing medium and PCR verified for *rad21nc* or *rec8* genes (**Supplementary Figures S3, S4**, respectively). Three confirmed

independent mutants of $\Delta rad21nc$ (3, 10, and 18) and two independent $\Delta rec8$ mutants (1 and 12) were further used for the experiments below.



Mycelial growth and sporulation were analyzed for the mutants and control strains on PDA medium; no significant difference was found (**Figures 5A,B**). Next, mycelial growth of

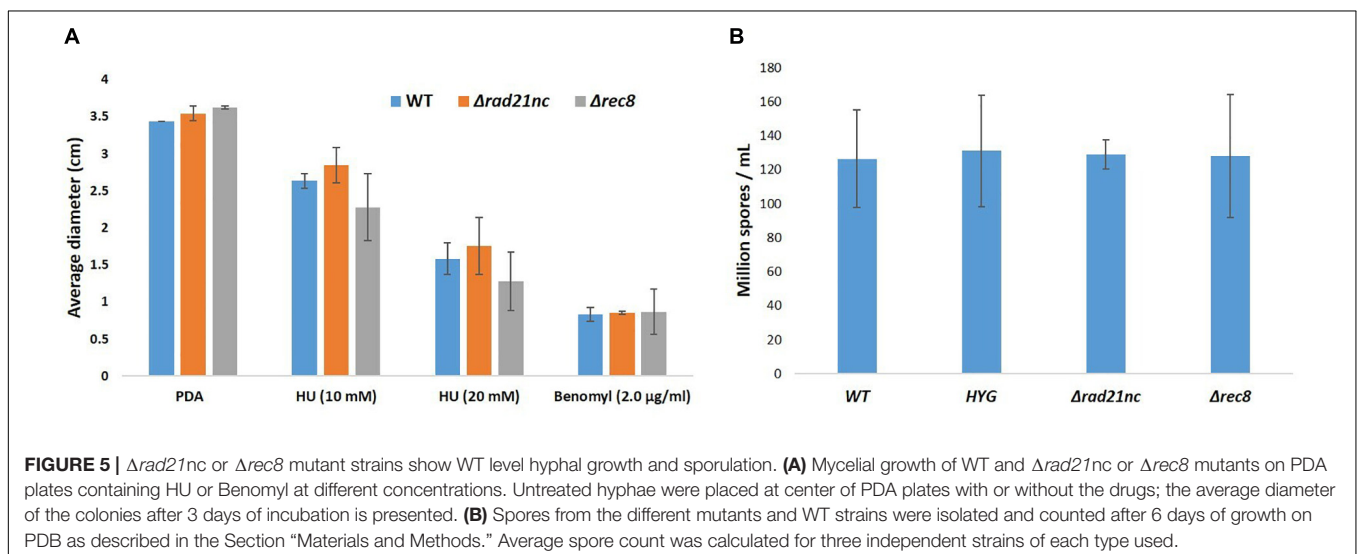
the mutants was also analyzed on PDA medium containing benomyl or HU. There was a slight decrease in the diameter of $\Delta rec8$ mutants in HU containing PDA plates as compared

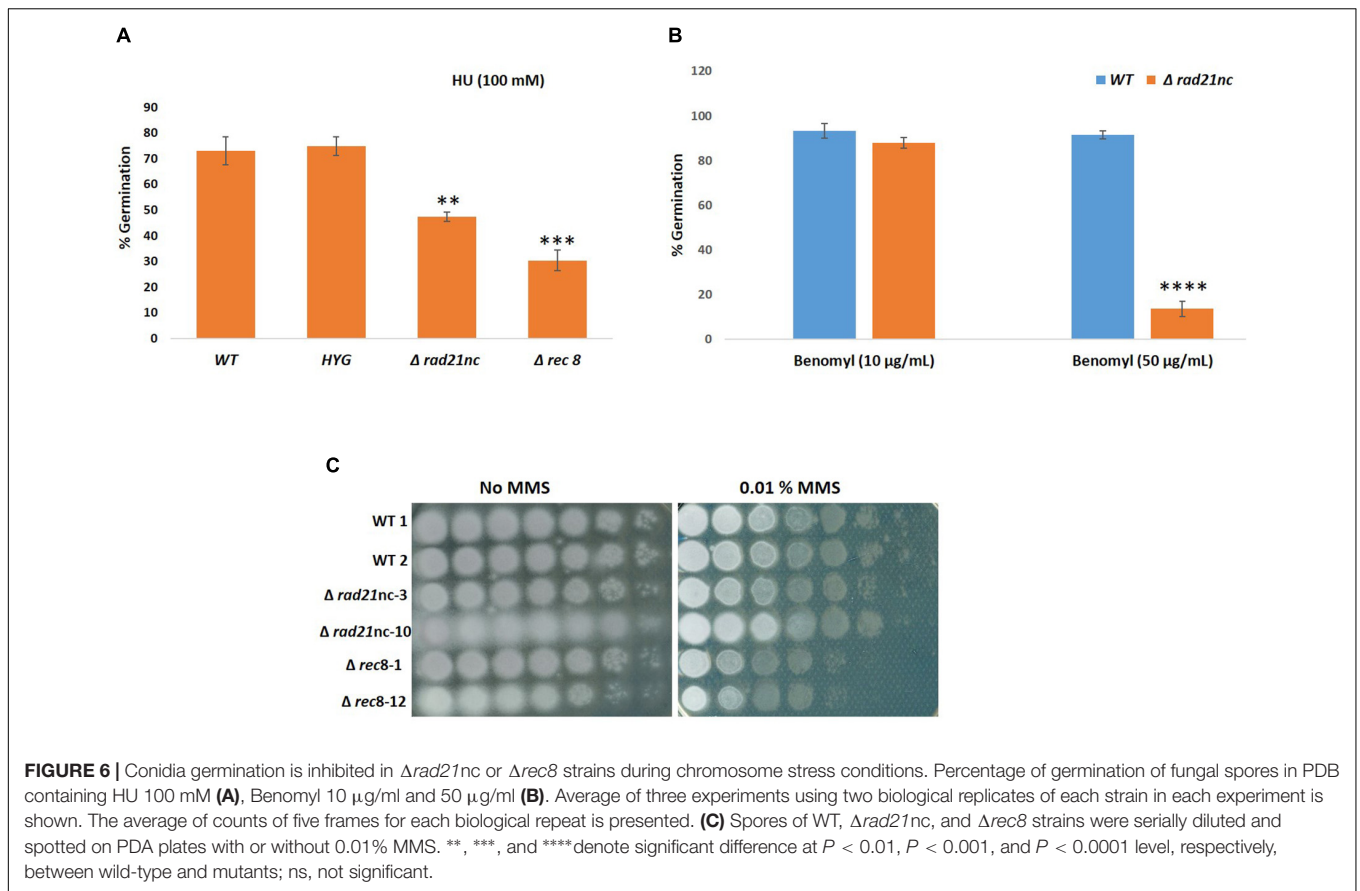


$\Delta rad21nc$ or $\Delta rec8$ Mutants Exhibit Delayed Germination Under Cell Cycle Perturbations

We analyzed the $\Delta rad21nc$ or $\Delta rec8$ mutant spore germination in different conditions. The germination of spores was measured in PDB medium as described under the Section “Materials and Methods”; no significant difference was observed between WT and the mutants. Spore germination under exposure of the mitosis inhibitor benomyl and the DNA replication inhibitor HU was measured. The $\Delta rad21nc$ and $\Delta rec8$ strains showed significantly lower germination rate under the 100 mM HU in PDB. The average percentage germination of WT fungal strains was 73.03% and *HYG* transformed strains it was 74.82%. Germination rate under these conditions was only 47.36% in $\Delta rad21nc$ and 30.36% in $\Delta rec8$ strains (**Figure 6A**). Similarly, when conidia were treated with 50 µg/ml benomyl, average percentage germination in WT strains was 91.46% and it was reduced to 13.68% in the $\Delta rad21nc$ mutant $\Delta rec8$ mutant showed inconsistent results (**Figure 6B**). In conclusion, we observed for $\Delta rad21nc$ and to lesser extent $\Delta rec8$ phenotypes that are directly linked to cell cycle perturbation. These results are in agreement with the notion that Rec8 and Rad21nc function

with WT strains but the growth difference was not significant (**Figure 5A**). No significant difference in the spore counts between WT, $\Delta rad21nc$ and $\Delta rec8$ strains was found (**Figure 5B**).





in alternative cohesin complexes since cohesin mutants are sensitive to benomyl and HU (Guacci et al., 1997; Aguilar et al., 2005; Heidinger-Pauli et al., 2010). We measured the expression of the different *rad21* paralogs under the same conditions of chromosome stress in the $\Delta rad21nc$ or $\Delta rec8$ strains. No dramatic increase in the expression of any of the paralogs was detected in the mutants comparing with WT strains. Small differences cannot be overruled due to the very low transcript levels of *rad21nc* and *rec8* (data not shown).

Sensitivity toward the DNA damaging agent MMS was analyzed for WT, $\Delta rad21nc$, or $\Delta rec8$ strains in a spot assay using serial dilutions (Figure 6C). $\Delta rec8$ mutant strains were more sensitive than WT to MMS by at least an order of magnitude. No sensitivity was observed in the $\Delta rad21nc$ mutant. Mutations in cohesin subunits are expected to increase mutagenicity. Measuring the rate of resistance to benomyl is a common forward mutation assay in fungi. We studied the rate of benomyl resistant

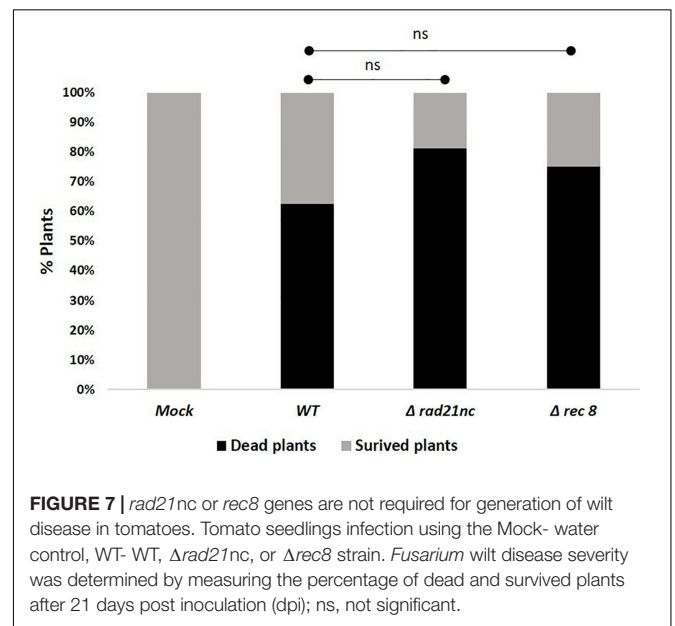


TABLE 1 | Increased rate of benomyl resistance in $\Delta rad21nc$ strains.

Genotype	Median Benomyl resistance rate	P-value (T-test WT: <i>rad21</i> mutant)
WT	2×10^{-6}	ND
$\Delta rad21nc$	44×10^{-6}	0.03
$\Delta rec8$	4×10^{-6}	0.48

mutant formation in WT, $\Delta rad21nc$, and $\Delta rec8$ strains. Nine cultures of each strain were grown in PDB for 5 days. Next, spores were collected and spread with appropriate dilutions on PDA plates and PDA plates containing benomyl (2 $\mu\text{g/ml}$). Colonies

were counted 2–3 days (PDA) or 6–7 days (benomyl) after plating. The rate of resistant mutants was calculated as previously described (Covo et al., 2014). While the median rates of WT and $\Delta rec8$ strains were similar, the rate of the $\Delta rad21nc$ was about 20 fold higher (P -value = 0.02 two tails T -test, **Table 1**).

Pathological Analysis of the $\Delta rad21nc$ or $\Delta rec8$ Mutant Strains

Finally, we determined the effect of a mutation in *rad21nc* or *rec8* on the ability of *F. oxysporum* f. sp. *lycopersici* to cause wilt disease in tomatoes. Plant infection was done using $\Delta rad21nc$ or $\Delta rec8$ strains on tomato seedlings. After 21 days post inoculation (dpi), we did not observe any significant change in the percentage of dead plants between the WT and mutant strains **Figure 7** and **Supplementary Figure S5**.

DISCUSSION

Rad21 as part of cohesin is essential for cell division and faithful transmission of chromosomes. It is also important for mitotic homologous recombination and gene expression (Onn et al., 2008). The model ascomycete fungi *S. cerevisiae*, *Schizosaccharomyces pombe*, *N. crassa*, and *A. nidulans* and most other sequenced species have two paralogs of *rad21*, one of them, *rec8* is supposed to function in homologous recombination during meiosis (Nasmyth and Haering, 2005, 2009). In some organisms there are more than two *rad21* paralogs; in all examined cases these paralogs had at least some non-overlapping functions (Bhatt et al., 1999; Severson et al., 2009; Ishiguro et al., 2011; da Costa-Nunes et al., 2014; Severson and Meyer, 2014). In an attempt to identify *F. oxysporum*-specific chromosome biology proteins we have found a non-conserved Rad21 paralog in few hypocreales species. Due to the small number of species that encode for Rad21nc it is hard to describe its evolution trajectory in high confidence. However, evidence lead to scenario of gene duplication after the divergence of *Trichoderma* species and before the divergence of *Stachybotrys* species from *F. solani* – followed by loss of the gene in most Fusarium species. This is based on the fact that the Rad21nc is found both in *F. oxysporum* and *F. nygamai* which is part of the *F. fujikuroi* species complex (**Figure 1**). The comparison of the sequences between the conserved and non-conserved *rad21* paralogs shows that the non-conserved one retains some classic α -kleisins domains (Smc1, Smc3 binding) (**Figure 2**). This may indicate that Rad21nc functions as part of a cohesion complex.

We analyzed the deletion strains of *rad21nc* or *rec8* gene. $\Delta rad21nc$ or $\Delta rec8$ mutant were similar to WT regarding sporulation and radial growth. We observed decrease in germination of the spores under the cell cycle stresses (**Figure 6**). HU induces DNA replication stress while benomyl activates the G2/M checkpoint. The sensitivity of *rad21nc* to these drugs suggests that *rad21nc* supports chromosome transmission or functions in a chromosome transmission checkpoint response. The germination of $\Delta rec8$ strains under HU stress and colony formation during MMS exposure are lower than WT cells suggesting a role in homologous recombinational repair as

recently described for Rec8 from *Ustilago maydis* (de Sena-Tomás et al., 2011; Sutherland and Holloman, 2018). Yet, a role in cell cycle control and non homologous recombination is also possible. The phenotypes of $\Delta rec8$ and $\Delta rad21nc$ strains are surprising since the expression of the two genes is very low even under HU and benomyl exposures (**Figure 4**). A probable explanation to how low amounts of a cohesin subunit may affect cells could be the fact that Rad21nc does not encode for a full separase domain. It is possible that few cohesin molecules associated with Rad21nc are evicted from chromosome in an alternative way that is needed for proper chromosome segregation in *F. oxysporum* under unique conditions.

Further studies are very much required to analyze the specific roles of the different Rad21 paralogs in fungal life cycle. Understanding the role of alternative cohesin complexes in *F. oxysporum* and other species will further open new dimensions for understanding the pathogen population genetics and genome evolution.

AUTHOR CONTRIBUTIONS

SC, MP, and YA designed the project and collected the initial data. SC, MP, and VB conducted the experiments. SC, MP, EH-C, and IO analyzed the data. SC, MP, and IO wrote the manuscript.

FUNDING

This research was supported by the Israel Science Foundation (ISF-211/16 to SC and ISF-1099/16 to IO).

SUPPLEMENTARY MATERIAL

The Supplementary Material for this article can be found online at: <https://www.frontiersin.org/articles/10.3389/fmicb.2019.01370/full#supplementary-material>

FIGURE S1 | A diagram explaining the strategy for the generation of the split marker cassette of *rad21nc* or *rec8*. The primer IDs' match the ones provided in **Supplementary Table S2**.

FIGURE S2 | Sequence alignment of *F. oxysporum* Rad21 and Rad21nc. Alignment was generated by using ClustalX2.

FIGURE S3 | Screening for $\Delta rad21nc$ transformants. **(A)** Confirmation of disruption of the *rad21nc* open reading frame using hygromycin resistant cassettes. PCR was used to amplify full length locus in wild type (WT) (2.0 kb), and the deleted locus (2.3 kb) using the P11 and P12 primers. 1 kb–1 kb marker (GeneDirex), WT- untransformed control, 1-18 are putative fungal transformants. **(B)** Amplification of the *rad21nc* ORF fragment using P1 and P13 primers, true mutants do not show amplification. 1 kb–1 kb marker (GeneDirex), W1, W2, and W3- untransformed control, 1-18 are putative fungal transformants. Transformants 3, 5, 6, 10, and 18 are true deleted strains for *rad21nc* locus.

FIGURE S4 | Screening for $\Delta rec8$ transformants. Confirmation of disruption of the *rec8* open reading frame using hygromycin resistant cassettes **(A)** Amplification of full length *rec8* locus in WT (2.5 kb) and the deleted locus (2.1 kb) using the P11 and P12 primers. 1 kb–1 kb marker (GeneDirex), W1 and W2 – untransformed control, 1-20 are putative fungal transformants. **(B)** Amplification of the *rec8* ORF using P11 and P13 primers, true mutants do not show amplification. 1 kb–1 kb marker (GeneDirex), W1 and W2 – untransformed control, 1-20 are putative fungal transformants. Transformants 1 and 12 are true deleted strains for *rec8* locus.

FIGURE S5 | Tomato wilt disease caused by *F. oxysporum* strains mutated in *rec8* or *rad21nc*. Tomato plants infected with WT, $\Delta rad21nc$, or $\Delta rec8$ fungal strains and water control (mock) after 21 dpi under controlled growth condition as described under the Section “Materials and Methods.”

TABLE S1 | 90 DNA Repair proteins that were used to build the species tree that is presented in **Figure 1**.

TABLE S2 | Primers used in the study.

REFERENCES

- Aguilar, C., Davidson, C., Dix, M., Stead, K., Zheng, K., Hartman, T., et al. (2005). Topoisomerase II suppresses the temperature sensitivity of *Saccharomyces cerevisiae* *pds5* mutants, but not the defect in sister chromatid cohesion. *Cell Cycle* 4, 1294–1304. doi: 10.4161/cc.4.9.1997
- Bae, Y. S., and Knudsen, G. R. (2000). Cotransformation of *Trichoderma harzianum* with beta-D-Glucuronidase and Green Fluorescent Protein genes provides a useful tool for monitoring fungal growth and activity in natural soils. *Appl. Environ. Microbiol.* 66, 810–815. doi: 10.1128/aem.66.2.810-815.2000
- Bai, X., Peirson, B. N., Dong, F., Xue, C., and Makaroff, C. A. (1999). Isolation and characterization of SYN1, a RAD21-like gene essential for meiosis in *Arabidopsis*. *Plant Cell* 11, 417–430. doi: 10.1105/tpc.11.3.417
- Bhatt, A. M., Lister, C., Page, T., Frasz, P., Findlay, K., Jones, G. H., et al. (1999). The DIF1 gene of *Arabidopsis* is required for meiotic chromosome segregation and belongs to the REC8/RAD21 cohesin gene family. *Plant J.* 19, 463–472. doi: 10.1046/j.1365-3113.1999.00548.x
- Bolaños-Villegas, P., De, K., Pradillo, M., Liu, D., and Makaroff, C. A. (2017). In favor of establishment: regulation of chromatid cohesion in plants. *Front. plant sci.* 8:846. doi: 10.3389/fpls.2017.00846
- Bose, T., and Gerton, J. L. (2010). Cohesinopathies, gene expression, and chromatin organization. *J. Cell Biol.* 189, 201–210. doi: 10.1083/jcb.200912129
- Catlett, N. L., Lee, B.-N., Yoder, O. C., and Turgeon, B. G. (2003). Split-Marker recombination for efficient targeted deletion of fungal genes. *Fungal Genet. Newsl.* 50, 9–11. doi: 10.4148/1941-4765.1150
- Covo, S., Ma, W., Westmoreland, J. W., Gordenin, D. A., and Resnick, M. A. (2012). Understanding the origins of UV-induced recombination through manipulation of sister chromatid cohesion. *Cell Cycle* 11, 3937–3944. doi: 10.4161/cc.21945
- Covo, S., Puccia, C. M., Argueso, J. L., Gordenin, D. A., and Resnick, M. A. (2014). The sister chromatid cohesion pathway suppresses multiple chromosome gain and chromosome amplification. *Genetics* 196, 373–384. doi: 10.1534/genetics.113.159202
- Covo, S., Westmoreland, J. W., Gordenin, D. A., and Resnick, M. A. (2010). Cohesin is limiting for the suppression of dna damage-induced recombination between homologous chromosomes. *PLoS Genet.* 6:e1001006. doi: 10.1371/journal.pgen.1001006
- da Costa-Nunes, J. A., Bhatt, A. M., O’Shea, S., West, C. E., Bray, C. M., Grossniklaus, U., et al. (2006). Characterization of the three *Arabidopsis thaliana* RAD21 cohesins reveals differential responses to ionizing radiation. *J. Exp. Bot.* 57, 971–983. doi: 10.1093/jxb/erj083
- da Costa-Nunes, J. A., Capitão, C., Kozak, J., Costa-Nunes, P., Ducasa, G. M., Pontes, O., et al. (2014). The AtRAD21.1 and AtRAD21.3 *Arabidopsis* cohesins play a synergistic role in somatic DNA double strand break damage repair. *BMC Plant Biol.* 14:353. doi: 10.1186/s12870-014-0353-9
- de Sena-Tomás, C., Fernández-Álvarez, A., Holloman, W. K., and Pérez-Martín, J. (2011). The DNA damage response signaling cascade regulates proliferation of the phytopathogenic fungus *Ustilago maydis* in planta. *Plant Cell* 23, 1654–1665. doi: 10.1105/tpc.110.082552
- Dean, R., Dean, R., Van Kan, J. A., Pretorius, Z. A., Hammond-Kosack, K. E., Di Pietro, A., et al. (2012). The Top 10 fungal pathogens in molecular plant pathology. *Mol. Plant Pathol* 13, 414–430. doi: 10.1111/j.1364-3703.2011.00783.x
- Di Pietro, A., García-MacEira, F. I., Męglec, E., and Roncero, M. I. (2001). A MAP kinase of the vascular wilt fungus *Fusarium oxysporum* is essential for root penetration and pathogenesis. *Mol. Microbiol.* 39, 1140–1152. doi: 10.1111/j.1365-2958.2001.02307.x
- Di Pietro, A., Isabel, M., and Roncero, G. (1998). Cloning, expression, and role in pathogenicity of *pg1* encoding the major extracellular endopolygalacturonase of the vascular wilt pathogen *Fusarium oxysporum*. *Mol. Plant Microbe Interact* 11, 91–98. doi: 10.1094/mpmi.1998.11.2.91
- Dong, F., Cai, X., and Makaroff, C. A. (2001). Cloning and characterization of two *Arabidopsis* genes that belong to the RAD21/REC8 family of chromosome cohesin proteins. *Gene* 271, 99–108. doi: 10.1016/s0378-1119(01)00499-1
- Gligoris, T. G., Scheinost, J. C., Bürmann, F., Petela, N., Chan, K. L., Uluocak, P., et al. (2014). Closing the cohesin ring: structure and function of its Smc3-kleisin interface. *Science* 346, 963–967. doi: 10.1126/science.1256917
- Goldman, G. H., and Kafer, E. (2004). *Aspergillus nidulans* as a model system to characterize the DNA damage response in eukaryotes. *Fungal Genet. Biol.* 41, 428–442. doi: 10.1016/j.fgb.2003.12.001
- Guacci, V., Koshland, D., and Strunnikov, A. (1997). A direct link between sister chromatid cohesion and chromosome condensation revealed through the analysis of MCD1 in *S. cerevisiae*. *Cell* 91, 47–57. doi: 10.1016/s0092-8674(01)80008-8
- Haering, C. H., Löwe, J., Hochwagen, A., and Nasmyth, K. (2002). Molecular architecture of SMC proteins and the yeast cohesin complex. *Mol. Cell* 9, 773–788. doi: 10.1016/s1097-2765(02)00515-4
- Haering, C. H., Schoffnegger, D., Nishino, T., Helmhart, W., Nasmyth, K., and Löwe, J. (2004). Structure and Stability of Cohesin’s Smc1-Kleisin Interaction. *Mol. Cell* 15, 951–964. doi: 10.1016/j.molcel.2004.08.030
- Heidinger-Pauli, J. M., Mert, O., Davenport, C., Guacci, V., and Koshland, D. (2010). Systematic reduction of cohesin differentially affects chromosome segregation, condensation, and DNA repair. *Curr. Biol.* 20, 957–963. doi: 10.1016/j.cub.2010.04.018
- Hongsanan, S., Maharachchikumbura, S. S., Hyde, K. D., Samarakoon, M. C., Jeewon, R., Zhao, Q., et al. (2017). An updated phylogeny of Sordariomycetes based on phylogenetic and molecular clock evidence. *Fungal Divers.* 84, 25–41. doi: 10.1007/s13225-017-0384-2
- Ishiguro, K., Kim, J., Fujiyama-Nakamura, S., Kato, S., and Watanabe, Y. (2011). A new meiosis-specific cohesin complex implicated in the cohesin code for homologous pairing. *EMBO Rep.* 12, 267–275. doi: 10.1038/embor.2011.2
- Kagey, M. H., Newman, J. J., Bilodeau, S., Zhan, Y., Orlando, D. A., van Berkum, N. L., et al. (2010). Mediator and cohesin connect gene expression and chromatin architecture. *Nature* 467, 430–435. doi: 10.1038/nature09380
- Kakui, Y., and Uhlmann, F. (2018). SMC complexes orchestrate the mitotic chromatin interaction landscape. *Curr. Genet.* 64, 335–339. doi: 10.1007/s00294-017-0755-y
- Katan, J., and Ausher, R. (1974). Distribution of race 2 of *Fusarium oxysporum* f. *sp.lycopersici* in tomato fields in Israel. *Phytoparasitica* 2, 83–90. doi: 10.1007/bf02980292
- Katoh, K., Asimenos, G., and Toh, H. (2009). “Multiple Alignment of DNA Sequences with MAFFT,” in *Bioinformatics for DNA Sequence Analysis. Methods in Molecular Biology (Methods and Protocols)*, Vol. 537, ed. D. Posada (New York, NY: Humana Press), 39–64. doi: 10.1007/978-1-59745-251-9_3
- Kim, K. P., Weiner, B. M., Zhang, L., Jordan, A., Dekker, J., and Kleckner, N. (2010). Sister cohesion and structural axis components mediate homolog bias of meiotic recombination. *Cell* 143, 924–937. doi: 10.1016/j.cell.2010.11.015
- Larkin, M. A., Blackshields, G., Brown, N. P., Chenna, R., Chenna, R., McGettigan, P. A., et al. (2007). Clustal W and Clustal X version 2.0. *Bioinformatics* 23, 2947–2948. doi: 10.1093/bioinformatics/btm404
- Lengronne, A., Katou, Y., Mori, S., Yokobayashi, S., Kelly, G. P., Itoh, T., et al. (2004). Cohesin relocation from sites of chromosomal loading to places of convergent transcription. *Nature* 430, 573–578. doi: 10.1038/nature02742
- Li, Y., Huang, W., Niu, L., Umbach, D. M., Covo, S., and Li, L. (2013). Characterization of constitutive CTCF/cohesin loci: a possible role in establishing topological domains in mammalian genomes. *BMC Genomics* 14:553. doi: 10.1186/1471-2164-14-553
- Livak, K. J., and Schmittgen, T. D. (2001). Analysis of relative gene expression data using real-time quantitative PCR and the 2⁻ΔΔCT method. *Methods* 25, 402–408. doi: 10.1006/meth.2001.1262
- Ma, L. J., Does, H. C., van der Borkovich, K. A., Coleman, J. J., Marie-Josée, D., Pietro, V., et al. (2010). Comparative genomics reveals mobile pathogenicity chromosomes in *Fusarium*. *Nature* 464, 367–373. doi: 10.1038/nature08850

- Ma, L. J., Geiser, D. M., Proctor, R. H., Rooney, A. P., O'Donnell, K., Trail, F., et al. (2013). Fusarium pathogenomics. *Annu. Rev. Microbiol.* 67, 399–416. doi: 10.1146/annurev-micro-092412-155650
- Moradi, S., Sanjarian, F., Safaie, N., Mousavi, A., Reza, G., and Khaniki, B. (2013). A modified method for transformation of *Fusarium graminearum*. *J. Crop Prot.* 2, 297–304. doi: 10.1016/j.fgb.2012.05.008
- Nakayashiki, H., Hanada, S., Quoc, N. B., Kadotani, N., Tosa, Y., and Mayama, S. (2005). RNA silencing as a tool for exploring gene function in ascomycete fungi. *Fungal Genet. Biol.* 42, 275–283. doi: 10.1016/j.fgb.2005.01.002
- Nasmyth, K., and Haering, C. H. (2005). The structure and function of Smc and Kleisin complexes. *Annu. Rev. Biochem.* 74, 595–648. doi: 10.1146/annurev-biochem.74.082803.133219
- Nasmyth, K., and Haering, C. H. (2009). Cohesin: its roles and mechanisms. *Annu. Rev. Genet.* 43, 525–558. doi: 10.1146/annurev-genet-102108-134233
- Onn, I., Heidinger-Pauli, J. M., Guacci, V., Ünal, E., and Koshland, D. E. (2008). Sister chromatid cohesion: a simple concept with a complex reality. *Annu. Rev. Cell Dev. Biol.* 24, 105–129. doi: 10.1146/annurev.cellbio.24.110707.175350
- Palecek, J. J., and Gruber, S. (2015). Kite Proteins: a superfamily of smc/kleisin partners conserved across bacteria, archaea, and eukaryotes. *Structure* 23, 2183–2190. doi: 10.1016/j.str.2015.10.004
- Ramamoorthy, V., Govindaraj, L., Dhanasekaran, M., Vetrivel, S., Kumar, K. K., and Ebenezer, E. (2015). Combination of driselase and lysing enzyme in one molar potassium chloride is effective for the production of protoplasts from germinated conidia of *Fusarium verticillioides*. *J. Microbiol. Methods* 111, 127–134. doi: 10.1016/j.mimet.2015.02.010
- Roy, A., Kucukural, A., and Zhang, Y. (2010). I-TASSER: a unified platform for automated protein structure and function prediction. *Nat. Protoc.* 5, 725–738. doi: 10.1038/nprot.2010.5
- Schneider, C. A., Rasband, W. S., and Eliceiri, K. W. (2012). NIH Image to ImageJ: 25 years of image analysis. *Nat. Methods* 9, 671–675. doi: 10.1038/nmeth.2089
- Sela, I., Ashkenazy, H., Katoh, K., and Pupko, T. (2015). GUIDANCE2: accurate detection of unreliable alignment regions accounting for the uncertainty of multiple parameters. *Nucleic Acids Res.* 43, W7–W14. doi: 10.1093/nar/gkv318
- Severson, A. F., Ling, L., van Zuylen, V., and Meyer, B. J. (2009). The axial element protein HTP-3 promotes cohesin loading and meiotic axis assembly in *C. elegans* to implement the meiotic program of chromosome segregation. *Genes Dev.* 23, 1763–1778. doi: 10.1101/gad.1808809
- Severson, A. F., and Meyer, B. J. (2014). Divergent kleisin subunits of cohesin specify mechanisms to tether and release meiotic chromosomes. *eLife* 3:e03467. doi: 10.7554/eLife.03467
- Sjögren, C., and Nasmyth, K. (2001). Sister chromatid cohesion is required for postreplicative double-strand break repair in *Saccharomyces cerevisiae*. *Curr. Biol.* 11, 991–995. doi: 10.1016/s0960-9822(01)00271-8
- Spencer, F., Gerring, S. L., Connelly, C., and Hieter, P. (1990). Mitotic chromosome transmission fidelity mutants in *Saccharomyces cerevisiae*. *Genetics* 124, 237–249.
- Stamatakis, A. (2014). RAxML version 8: a tool for phylogenetic analysis and post-analysis of large phylogenies. *Bioinformatics* 30, 1312–1313. doi: 10.1093/bioinformatics/btu033
- Stirling, P. C., Bloom, M. S., Solanki-Patil, T., Smith, S., Sipahimalani, P., Li, Z., et al. (2011). The complete spectrum of yeast chromosome instability genes identifies candidate CIN cancer genes and functional roles for ASTRA complex components. *PLoS Genet.* 7:e1002057. doi: 10.1371/journal.pgen.1002057
- Sutherland, J. H., and Holloman, W. K. (2018). Loss of cohesin subunit Rec8 switches Rad51 mediator dependence in resistance to formaldehyde toxicity in *Ustilago maydis*. *Genetics* 210, 559–572. doi: 10.1534/genetics.118.301439
- Uhlmann, F., Lottspeich, F., and Nasmyth, K. (1999). Sister-chromatid separation at anaphase onset is promoted by cleavage of the cohesin subunit Scc1. *Nature* 400, 37–42. doi: 10.1038/21831
- Ünal, E., Arbel-Eden, A., Sattler, U., Shroff, R., Lichten, M., Haber, J. E., et al. (2004). dna damage response pathway uses histone modification to assemble a double-strand break-specific cohesin domain. *Mol. Cell* 16, 991–1002. doi: 10.1016/j.molcel.2004.11.027
- van Ruiten, M. S., and Rowland, B. D. (2018). SMC complexes: universal DNA looping machines with distinct regulators. *Trends Genet.* 34, 477–487. doi: 10.1016/j.tig.2018.03.003
- Vlaardingerbroek, I., Beerens, B., Rose, L., Fokkens, L., Cornelissen, B. J. C., and Rep, M. (2016). Exchange of core chromosomes and horizontal transfer of lineage-specific chromosomes in *Fusarium oxysporum*. *Environ. Microbiol.* 18, 3702–3713. doi: 10.1111/1462-2920.13281
- Watanabe, Y., and Nurse, P. (1999). Cohesin Rec8 is required for reductional chromosome segregation at meiosis. *Nature* 400, 461–464. doi: 10.1038/22774
- Yang, J., Yan, R., Roy, A., Xu, D., Poisson, J., and Zhang, Y. (2015). The I-TASSER suite: protein structure and function prediction. *Nat. Methods* 12, 7–8. doi: 10.1038/nmeth.3213
- Yang, Z. (1994). Maximum likelihood phylogenetic estimation from DNA sequences with variable rates over sites: approximate methods. *J. Mol. Evol.* 39, 306–314. doi: 10.1007/BF00160154
- Yu, J.-H., Hamari, Z., Han, K.-H., Seo, J.-A., Reyes-Domínguez, Y., and Scazzocchio, C. (2004). Double-joint PCR: a PCR-based molecular tool for gene manipulations in filamentous fungi. *Fungal Genet. Biol.* 41, 973–981. doi: 10.1016/j.fgb.2004.08.001
- Zhang, Y. (2008). I-TASSER server for protein 3D structure prediction. *BMC Bioinformatics* 9:40. doi: 10.1186/1471-2105-9-40
- Zickler, D., and Kleckner, N. (1999). Meiotic chromosomes: integrating structure and function. *Ann. Rev. Genet.* 33, 603–754. doi: 10.1146/annurev.genet.33.1.603

Conflict of Interest Statement: The authors declare that the research was conducted in the absence of any commercial or financial relationships that could be construed as a potential conflict of interest.

Copyright © 2019 Pareek, Almog, Bari, Hazkani-Covo, Onn and Covo. This is an open-access article distributed under the terms of the Creative Commons Attribution License (CC BY). The use, distribution or reproduction in other forums is permitted, provided the original author(s) and the copyright owner(s) are credited and that the original publication in this journal is cited, in accordance with accepted academic practice. No use, distribution or reproduction is permitted which does not comply with these terms.